Stochastic Structural Dynamics Using Frequency Adaptive Basis Functions

A. Kundu and S. Adhikari

Abstract A novel Galerkin subspace projection scheme for structural dynamic systems with stochastic parameters is developed in this chapter. The fundamental idea is to solve the discretised stochastic damped dynamical system in the frequency domain by projecting the solution into a reduced subspace of eigenvectors of the underlying deterministic operator. The associated complex random coefficients are obtained as frequency-dependent quantities, termed as spectral functions. Different orders of spectral functions are proposed depending on the order of the terms retained in the expression. Subsequently, Galerkin weighting coefficients are employed to minimise the error induced due to the reduced basis and finite order spectral functions. The complex response quantity is explicitly expressed in terms of the spectral functions, eigenvectors and the Galerkin weighting coefficients. The statistical moments of the solution are evaluated at all frequencies including the resonance and antiresonance frequencies for a fixed value of damping. Two examples involving a beam and a plate with stochastic properties subjected to harmonic excitations are considered. The results are compared to direct Monte Carlo simulation and polynomial chaos expansion for different correlation lengths and variability of randomness.

Keywords Stochastic dynamics • Random field • Spectral decomposition • Karhunen-Loeve Expansion • Stochastic subspace

1 Introduction

The framework of the present work is the parametric uncertainty that is inherent in the mathematical models laid out to describe the governing equations of physical systems. These uncertainties may be intrinsic variability of physical quantities or a

A. Kundu (✉) • S. Adhikari
College of Engineering, Swansea University, Singleton Park SA2 8PP, UK
e-mail: a.kundu.577613@swansea.ac.uk

S. Chakraborty and G. Bhattacharya (eds.), *Proceedings of the International Symposium on Engineering under Uncertainty: Safety Assessment and Management (ISEUSAM - 2012)*,
DOI 10.1007/978-81-322-0757-3_10,

lack of knowledge about the physical behaviours of certain systems. As a result, though the recent advances in computational hardware has enabled the solution of very high resolution problems and even the sophisticated techniques of *a posteriori* error estimation [3], mesh adaptivity or the modelling error analysis has improved the confidence on results, yet these are not enough to determine the credibility of the numerical model.

There has been an increasing amount of research activities over the past three decades to model the governing partial differential equations within the framework of stochastic equations. We refer to few recent review papers [1, 8, 9]. After the discretisation of random fields and displacement fields, the equation of motion can be expressed by [2, 4, 5] a set of stochastic ordinary differential equations

$$\mathbf{M}(\theta)\,\ddot{\mathbf{u}}\,(\theta,\,t) + \mathbf{C}(\theta)\,\dot{\mathbf{u}}\,(\theta,\,t) + \mathbf{K}(\theta)\,\mathbf{u}(\theta,\,t) = \mathbf{f}_0(t) \tag{1}$$

where $\mathbf{M}(\theta) = \mathbf{M}_0 + \sum_{i=1}^{p_1} \mu i(\theta)\mathbf{M}_i \in \mathbb{R}^{n\times n}$ is the random mass matrix and $\mathbf{K}(\theta) = \mathbf{K}_0 + \sum_{i=1}^{p_2} vi(\theta)\mathbf{K}_i \in \mathbb{R}^{n\times n}$ is the random stiffness matrix along with $\mathbf{C}(\theta) \in \mathbb{R}^{n\times n}$ as the random damping matrix. The notation θ is used to denote the random sample space. Here, the mass and stiffness matrices have been expressed in terms of their deterministic components ($\mathbf{M_0}$ and $\mathbf{K_0}$) and the corresponding random contributions ($\mathbf{M_i}$ and $\mathbf{K}_i$) obtained from discretising the stochastic field with a finite number of random variables ($\mu_i(\theta)$ and $v_i(\theta)$) and their corresponding spatial basis functions. In the present work proportional damping is considered for which $\mathbf{C}(\theta) = \varsigma_1\mathbf{M}(\theta) + \varsigma_2\mathbf{K}(\theta)$, where ς_1 and ς_2 are deterministic scalars. For the harmonic analysis of the structural system considered in Eq. (1), it is represented in the frequency domain as

$$\left[-\omega^2\mathbf{M}(\theta) + i\omega\mathbf{C}(\theta) + \mathbf{K}(\theta)\right]\tilde{\mathbf{u}}(\theta,\,\omega) = \tilde{\mathbf{f}}_0(\omega) \tag{2}$$

where $\tilde{\mathbf{u}}(\theta,\,\omega)$ is the complex frequency domain system response amplitude and $\tilde{\mathbf{f}}_0(\omega)$ is the amplitude of the harmonic force.

Now we group the random variables associated with the mass and damping matrices of Eq. (1) as

$$\xi_i(\theta) = \mu_i(\theta) \quad for \quad i = 1, 2, \ldots, p_1$$
$$\text{and} \quad \xi_{i+p_1}(\theta) = v_i(\theta) \quad for \quad i = 1, 2, \ldots, p_2$$

Thus, the total number of random variables used to represent the mass and the stiffness matrices becomes $p = p_1 + p_2$. Following this, the expression for the linear structural system in Eq. (2) can be expressed as

$$\left(\mathbf{A}_0(\omega) + \sum_{i=1}^{p} \xi_i(\theta)\mathbf{A}_i(\omega)\right)\tilde{\mathbf{u}}(\omega,\theta) = \tilde{\mathbf{f}}_0(\omega) \tag{3}$$

where $\mathbf{A_o}$ and $\mathbf{A}_i \in \mathbb{C}^{n\times n}$ represent the complex deterministic and stochastic parts, respectively, of the mass, the stiffness and the damping matrices ensemble. For the case of proportional damping, the matrices $\mathbf{A}_o$ and $\mathbf{A}_i$ can be written as

$$\mathbf{A}_0(\omega) = \left[-\omega^2 + i\omega\varsigma_1\right]\mathbf{M}_0 + [i\omega\varsigma_2 + 1]\mathbf{K}_0 \tag{4}$$

and

$$\begin{aligned}\mathbf{A}_i(\omega) &= \left[-\omega^2 + i\omega\varsigma_1\right]\mathbf{M}_i \quad \text{for} \quad i = 1, 2, ..., p_1\\ \mathbf{A}_{i+p_1}(\omega) &= [i\omega\varsigma_2 + 1]\mathbf{K}_i \quad \textit{for} \quad i = 1, 2, ..., p_2\end{aligned} \tag{5}$$

The chapter has been arranged as follows. The projection theory in the vector space is developed in Sect. 2. In Sect. 3 an error minimisation approach in the Hilbert space is proposed. The idea of the reduced orthonormal vector basis is introduced in Sect. 4. Based on the theoretical results, a simple computational approach is shown in Sect. 5 where the proposed method of reduced orthonormal basis is applied to the stochastic mechanics of a Euler-Bernoulli beam. From the theoretical developments and numerical results, some conclusions are drawn in Sect. 6.

2 Spectral Decomposition in the Vector Space

Following the spectral stochastic finite-element method, or otherwise, an approximation to the solution stochastic system can be expressed as a linear combination of functions of random variables and deterministic vectors. Recently Nouy [6, 7] discussed the possibility of an optimal spectral decomposition. The aim is to use small number of terms to reduce the computation without losing the accuracy. We use the eigenvectors $\phi_k \in \mathbb{R}^n$ of the generalised eigenvalue problem

$$\mathbf{K}_0\phi_k = \lambda_k\mathbf{M}_0\phi_k; \quad k = 1, 2, ...n \tag{6}$$

Since the matrices $\mathbf{K_0}$ and $\mathbf{M_0}$ are symmetric and generally non-negative definite, the eigenvectors ϕ_k for $k = 1, 2, ...n$ form an orthonormal basis. Note that in principle, any orthonormal basis can be used. This choice is selected due to the analytical simplicity as will be seen later. For notational convenience, define the matrix of eigenvalues and eigenvectors

$$\lambda_0 = \text{diag}[\lambda_1, \lambda_2, \ldots, \lambda_n] \in \mathbb{R}^{n\times n} \quad \text{and} \quad \Phi = [\phi_1, \phi_2, \ldots, \phi_n] \in \mathbb{R}^{n\times n} \tag{7}$$

Eigenvalues are ordered in the ascending order so that $\lambda_1 < \lambda_2 < \ldots < \lambda_n$. Since Φ is an orthonormal matrix, we have $\Phi^{-1} = \Phi^T$ so that the following identities can easily be established:

$$\begin{aligned}\Phi^T\mathbf{A}_0\Phi &= \Phi^T\left(\left[-\omega^2 + i\omega\varsigma_1\right]\mathbf{M}_0 + [i\omega\varsigma_2 + 1]\mathbf{K}_0\right)\Phi\\ &= \left(-\omega^2 + i\omega\varsigma_1\right)\mathbf{I} + (i\omega\varsigma_2 + 1)\lambda_0\end{aligned}$$

which gives

$$\Phi^T \mathbf{A}_0 \Phi = \Lambda_0; \quad \mathbf{A}_0 = \Phi^{-T} \Lambda_0 \Phi^{-1} \quad \text{and} \quad \mathbf{A}_0^{-1} = \Phi \Lambda_0^{-1} \Phi^{-T} \tag{8}$$

where $\Lambda_0 = (-\omega^2 + i\omega\varsigma_1)\mathbf{I} + (i\omega\varsigma_2 + 1)\lambda_0$ and $\mathbf{I}$ is the identity matrix. Hence, Λ_0 can also be written as

$$\Lambda_0 = \text{diag}\left[\lambda_{0_1}, \lambda_{0_2}, \ldots, \lambda_{0_n}\right] \in \mathbb{C}^{n \times n} \tag{9}$$

where $\lambda_{0_j} = (-\omega^2 + i\omega\varsigma_1) + (i\omega\varsigma_2 + 1)\lambda_j$ and λ_j is defined in Eq. (7). We also introduce the transformations

$$\tilde{\mathbf{A}}_i = \Phi^T \mathbf{A}_i \Phi \in \mathbb{C}^{n \times n}; i = 0, 1, 2, \ldots, M \tag{10}$$

Note that $\tilde{\mathbf{A}}_i = \Lambda_0$ is a diagonal matrix and

$$\tilde{\mathbf{A}}_i = \Phi^{-T} \tilde{\mathbf{A}}_i \Phi^{-1} \in \mathbb{C}^{n \times n}; i = 0, 1, 2, \ldots, M \tag{11}$$

Suppose the solution of Eq. (3) is given by

$$\hat{\mathbf{u}}(\omega, \theta) = \left[\mathbf{A}_0(\omega) + \sum_{i=1}^{M} \xi_i(\theta) \mathbf{A}_i(\omega)\right]^{-1} \mathbf{f}_0(\omega) \tag{12}$$

Using Eqs. (7), (8), (9), (10), and (11) and the orthonormality of Φ, one has

$$\begin{aligned} \hat{\mathbf{u}}(\omega, \theta) &= \left[\Phi^{-T} \Lambda_0(\omega) \Phi^{-1} + \sum_{i=1}^{M} \xi_i(\theta) \Phi^{-T} \tilde{\mathbf{A}}_i \Phi^{-1}\right]^{-1} \mathbf{f}_0(\omega) \\ &= \Phi \Psi(\omega, \xi(\theta)) \Phi^{-T} \mathbf{f}_0(\omega) \end{aligned} \tag{13}$$

where

$$\Psi(\omega, \xi(\theta)) = \left[\Lambda_0(\omega) + \sum_{i=1}^{M} \xi_i(\theta) \tilde{\mathbf{A}}_i(\omega)\right]^{-1} \tag{14}$$

and the M-dimensional random vector

$$\xi(\theta) = \{\xi_1(\theta), \xi_2(\theta), \ldots, \xi_M(\theta)\}^T \tag{15}$$

Now we separate the diagonal and off-diagonal terms of the $\tilde{\mathbf{A}}_i$ matrices as

$$\tilde{\mathbf{A}}_i = \Lambda_i + \Delta_i, \quad i = 1, 2, \ldots, M \tag{16}$$

Here, the diagonal matrix

$$\Lambda_i = \text{diag}\left[\tilde{\mathbf{A}}_i\right] = \text{diag}\left[\lambda_{i_1}, \lambda_{i_2}, \ldots, \lambda_{i_n}\right] \in \mathbb{C}^{n\times n} \tag{17}$$

and the matrix containing only the off-diagonal elements $\Delta_i = \tilde{\mathbf{A}}_i - \Lambda_i$ is such that Trace $(\Delta_i) = 0$. Using these, from Eq. (14) one has

$$\Psi(\omega, \xi(\theta)) = \left[\underbrace{\Lambda_0(\omega) + \sum_{i=1}^{M} \xi_i(\theta)\Lambda_i(\omega)}_{\Lambda(\omega,\boldsymbol{\xi}(\theta))} + \underbrace{\sum_{i=1}^{M} \xi_i(\theta)\Delta_i(\omega)}_{\Delta(\omega,\boldsymbol{\xi}(\theta))}\right]^{-1} \tag{18}$$

where $\Lambda(\omega, \boldsymbol{\xi}(\theta)) \in \mathbb{C}^{n\times n}$ is a diagonal matrix and $\Delta(\omega, \boldsymbol{\xi}(\theta))$ is an off-diagonal only matrix. In the subsequent expressions, we choose to omit the inclusion of frequency dependence of the individual matrices for the sake of notational simplicity, so that $\Psi(\omega, \boldsymbol{\xi}(\theta)) \equiv \Psi(\boldsymbol{\xi}(\theta))$ and so on. Hence, we rewrite Eq. (18) as

$$\Psi(\boldsymbol{\xi}(\theta)) = \left[\Lambda(\boldsymbol{\xi}(\theta))\left[\mathbf{I}_n + \Lambda^{-1}(\boldsymbol{\xi}(\theta))\Delta(\boldsymbol{\xi}(\theta))\right]\right]^{-1} \tag{19}$$

The above expression can be represented using a Neumann type of matrix series [10] as

$$\Psi(\boldsymbol{\xi}(\theta)) = \sum_{s=0}^{\infty} (-1)^s \left[\Lambda^{-1}(\boldsymbol{\xi}(\theta))\Delta(\boldsymbol{\xi}(\theta))\right]^s \Lambda^{-1}(\boldsymbol{\xi}(\theta)) \tag{20}$$

Taking an arbitrary r-th element of $\hat{\mathbf{u}}(\theta)$, Eq. (13) can be rearranged to have

$$\hat{u}_r(\theta) = \sum_{k=1}^{n} \Phi_{rk} \left(\sum_{j=1}^{n} \Psi_{kj}(\boldsymbol{\xi}(\theta)) \left(\phi_j^T \mathbf{f}_0 \right) \right) \tag{21}$$

Defining

$$\Gamma_k(\xi(\theta)) = \sum_{j=1}^{n} \Psi_{kj}(\boldsymbol{\xi}(\theta)) \left(\phi_j^T \mathbf{f}_0 \right) \tag{22}$$

and collecting all the elements in Eq. (21) for $r = 1,2,\ldots,n$, one has

$$\hat{\mathbf{u}}(\theta) = \sum_{k=1}^{n} \Gamma_k(\boldsymbol{\xi}(\theta))\phi_k \tag{23}$$

This shows that the solution vector $\hat{\mathbf{u}}(\theta)$ can be projected in the space spanned by ϕ_k.

3 Error Minimisation Using the Galerkin Approach

In Sec. 2 we derived the spectral functions such that a projection in an orthonormal basis converges to the exact solution in probability 1. The spectral functions are expressed in terms of a convergent infinite series. First, second- and higher-order spectral functions obtained by truncating the infinite series have been derived. We have also showed that they have the same functional form as the exact solution of Eq. (3). This motivates us to use these functions as 'trial functions' to construct the solution. The idea is to minimise the error arising due to the truncation. A Galerkin approach is proposed where the error is made orthogonal to the spectral functions.

We express the solution vector by the series representation

$$\hat{\mathbf{u}}(\theta) = \sum_{k=1}^{n} c_k \widehat{\Gamma}_k(\boldsymbol{\xi}(\theta))\phi_k \tag{24}$$

Here, the functions $\widehat{\Gamma}_k : \mathbb{C}^M \to \mathbb{C}$ are the spectral functions, and the constants $c_k \in \mathbb{C}$ need to be obtained using the Galerkin approach. The functions $\widehat{\Gamma_k}(\xi(\theta))$ can be the first-order, second-order or any higher-order spectral function (depending on the order of the expansion s in Eq. (20)) and are the complex frequency adaptive weighting coefficient of the eigenvectors introduced earlier in Eq. (6). Substituting the expansion of $\hat{\mathbf{u}}(\theta)$ in the linear system equation (3), the error vector can be obtained as

$$\varepsilon(\theta) = \left(\sum_{i=0}^{M} \mathbf{A}_i \xi_i(\theta)\right)\left(\sum_{k=1}^{n} c_k \widehat{\Gamma_k}(\boldsymbol{\xi}(\theta))\phi_k\right) - \mathbf{f}_0 \in \mathbb{C}^n \tag{25}$$

where $\xi_0 = 1$ is used to simplify the first summation expression. The expression (24) is viewed as a projection where $\left\{\widehat{\Gamma_k}(\boldsymbol{\xi}(\theta))\phi_k\right\} \in \mathbb{C}^n$ are the basis functions and c_k are the unknown constants to be determined. We wish to obtain the coefficients c_k using the Galerkin approach so that the error is made orthogonal to the basis functions, that is, mathematically

$$\varepsilon(\theta) \perp \left(\widehat{\Gamma}_j(\boldsymbol{\xi}(\theta))\phi_j\right) \quad \text{or} \quad \left\langle \widehat{\Gamma}_j(\boldsymbol{\xi}(\theta))\phi_j, \varepsilon(\theta) \right\rangle = 0 \; \forall \, j = 1, 2, \ldots, n \tag{26}$$

Here, $\langle \mathbf{u}(\theta), \mathbf{v}(\theta) \rangle = \int P(d\theta \mathbf{u}(\theta)\mathbf{v}(\theta))$ defines the inner product norm. Imposing this condition and using the expression of $\varepsilon(\theta)$ from Eq. (25), one has

$$E\left[\left(\widehat{\Gamma}_j(\boldsymbol{\xi}(\theta))\phi_j\right)^T \left(\sum_{i=0}^{M} \mathbf{A}_i \xi_i(\theta)\right)\left(\sum_{k=1}^{n} c_k \widehat{\Gamma_k}(\boldsymbol{\xi}(\theta))\phi_k\right) - \left(\widehat{\Gamma}_j(\boldsymbol{\xi}(\theta))\phi_j\right)^T \mathbf{f}_0\right] = 0 \tag{27}$$

Interchanging the $E[\bullet]$ and summation operations, this can be simplified to

$$\sum_{k=1}^{n}\left(\sum_{i=0}^{M}\left(\phi_j^T\mathbf{A}_i\phi_k\right)E\left[\xi_i(\theta)\widehat{\Gamma}_j^T(\boldsymbol{\xi}(\theta))\widehat{\Gamma}_k(\boldsymbol{\xi}(\theta))\right]\right)c_k = E\left[\widehat{\Gamma}_j^T(\boldsymbol{\xi}(\theta))\right]\left(\phi_j^T\mathbf{f}_o\right) \quad (28)$$

or

$$\sum_{k=1}^{n}\left(\sum_{i=0}^{M}\widetilde{A}_{i_{jk}}D_{ijk}\right)c_k = b_j \quad (29)$$

Defining the vector $\mathbf{c} = \{c_1, c_2, \ldots, c_n\}^T$, these equations can be expressed in a matrix form as

$$\mathbf{S}\,\mathbf{c} = \mathbf{b} \quad (30)$$

with

$$S_{jk} = \sum_{i=0}^{M}\widetilde{A}_{i_{jk}}D_{ijk}; \quad \forall j,k = 1,2,\ldots,n \quad (31)$$

where

$$\widetilde{A}_{i_{jk}} = \phi_j^T\mathbf{A}_i\phi_k, \quad (32)$$

$$D_{ijk} = E\left[\xi_i(\theta)\widehat{\Gamma}_j^T(\boldsymbol{\xi}(\theta))\widehat{\Gamma}_k(\boldsymbol{\xi}(\theta))\right] \quad (33)$$

and

$$b_j = E\left[\widehat{\Gamma}_j^T(\boldsymbol{\xi}(\theta))\right]\left(\phi_j^T\mathbf{f}_o\right) \quad (34)$$

Higher-order spectral functions can be used to improve the accuracy and convergence of the series (24). This will be demonstrated in the numerical examples later in the chapter.

4 Model Reduction Using a Reduced Number of Basis

The Galerkin approach proposed in the previous section requires the solution of $n \times n$ algebraic equations. Although in general this is smaller compared to the polynomial chaos approach, the computational cost can still be high for large n as the coefficient matrix is in general a dense matrix. The aim of this section is to reduce it further so that, in addition to large number of random variables, problems with large degrees of freedom can also be solved efficiently.

Suppose the eigenvalues of $\mathbf{A}_0$ are arranged in an increasing order such that

$$\lambda_{01} < \lambda_{02} < \ldots < \lambda_{0n} \tag{35}$$

From the expression of the spectral functions, observe that the eigenvalues appear in the denominator:

$$\widehat{\Gamma}_k^{(1)}(\boldsymbol{\xi}(\theta)) = \frac{\phi_k^T \mathbf{f}_0}{\lambda_{0k} + \sum_{i=1}^{M} \xi_i(\theta)\lambda_{i_k}} \tag{36}$$

The numerator $\left(\phi_k^T \mathbf{f}_0\right)$ is the projection of the force on the deformation mode. Since the eigenvalues are arranged in an increasing order, the denominator of $\left|\Gamma_{k+r}^{(1)}(\boldsymbol{\xi}(\theta))\right|$ is larger than the denominator of $\left|\Gamma_k^{(1)}(\boldsymbol{\xi}(\theta))\right|$ according a suitable measure. The numerator $\left(\phi_k^T \mathbf{f}_0\right)$ depends on the nature of forcing and the eigenvectors. Although this quantity is deterministic, in general an ordering cannot be easily established for different values of k. Because all the eigenvectors are normalised to unity, it is reasonable to consider that $\left(\phi^T{}_k f_0\right)$ does not vary significantly for different values of k. Using the ordering of the eigenvalues, one can select a small number ϵ such that $\lambda_1/\lambda_q < \epsilon$ for some value of q, where λ_j is the eigenvalue of the generalised eigenvalue problem defined in Eq. (6). Based on this, we can approximate the solution using a truncated series as

$$\hat{\mathbf{u}}(\theta) \approx \sum_{k=1}^{q} c_k \widehat{\Gamma_k}(\boldsymbol{\xi}(\theta))\phi_k \tag{37}$$

where c_k, $\widehat{\Gamma}_k(\boldsymbol{\xi}(\theta))$ and are obtained following the procedure described in the previous section by letting the indices j, k only up to q in Eqs. (31) and (32). The accuracy of the series (37) can be improved in two ways, namely, (a) by increasing the number of terms q or (b) by increasing the order of the spectral functions $\widehat{\Gamma_k}(\boldsymbol{\xi}(\theta))$. Once the samples of $\mathbf{u} = (\theta)$ are generated, the statistics can be obtained using standard procedures.

5 Illustrative Application: The Stochastic Mechanics of a Euler-Bernoulli Beam

In this section we apply the computational method to a cantilever beam with stochastic bending modulus. We assume that the bending modulus is a homogeneous stationary Gaussian random field of the form

$$EI(x,\theta) = EI_0(1 + a(x,\theta)) \tag{38}$$

where x is the coordinate along the length of the beam, EI_0 is the estimate of the mean bending modulus and $a(x,\theta)$ is a zero mean stationary Gaussian random field. The autocorrelation function of this random field is assumed to be

$$C_a(x_1, x_2) = \sigma_a^2 e^{\frac{-(|x_1 - x_2|)}{\mu_a}} \tag{39}$$

where μ_a is the correlation length and σ_a is the standard deviation. We use the baseline parameters as the length $L = 1$ m, cross section $(b \times h)$ 39×5.93 mm^2 and Young's modulus $E = 2 \times 10^{11}$ Pa.

In study we consider deflection of the tip of the beam under harmonic loads of amplitude $\tilde{f}_0 = 1.0N$. The correlation length considered in this numerical study is $\mu_a = L/2$. The number of terms retained (M) in the Karhunen-Loeve expansion is selected such that $v_M/v_1 = 0.01$ in order to retain 90% of the variability. For this correlation length, the number of terms M comes to 18. For the finite element discretisation, the beam is divided into 40 elements. Standard four degrees of freedom Euler-Bernoulli beam model is used [11]. After applying the fixed boundary condition at one edge, we obtain the number of degrees of freedom of the model to be $n = 80$.

5.1 Results

The proposed method has been compared with a direct Monte Carlo simulation (MCS), where both have been performed with 10,000 samples. For the direct MCS, Eq. (12) is solved for each sample, and the mean and standard deviation is derived by assembling the responses. The calculations have been performed for all the four values of σ_a to simulate increasing uncertainty. This is done to check the accuracy of the proposed method against the direct MCS results for varying degrees of uncertainty.

Figure 1a presents the ratio of the eigenvalues of the generalised eigenvalue problem (6) for which the ratio of the eigenvalues is taken with the first eigenvalue. We choose the reduced basis of the problem based on $\lambda_1/\lambda_q < \in$, where $e = 0.01$, and they are highlighted in the figure. Figure 1b shows the frequency domain response of the deterministic system for both damped and undamped conditions. We have applied a constant modal damping matrix with the damping coefficient $\alpha = 0.02$ (which comes to 1% damping). It is also to be noted that the mass and damping matrices are assumed to be deterministic in nature, while it has to be emphasised that the approach is equally valid for random mass, stiffness and damping matrices. The frequency range of interest for the present study is 0–600 Hz with an interval of 2 Hz. In Fig. 1b, the tip deflection is shown on a log scale for a unit amplitude harmonic force input. The resonance peak amplitudes of the response of the undamped system definitely depend on the frequency resolution of the plot.

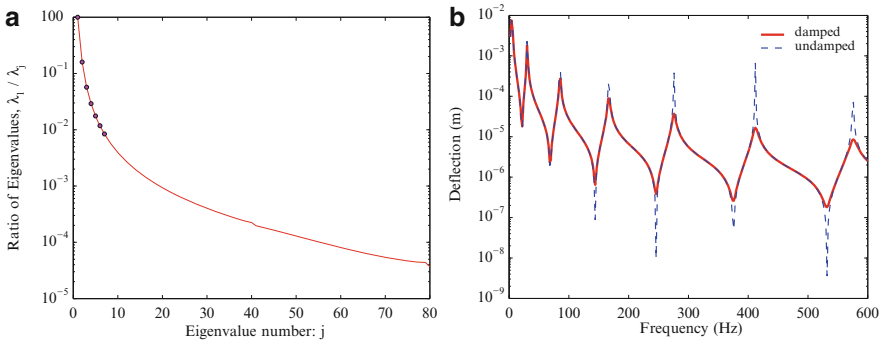

Fig. 1 The eigenvalues of the generalised eigenvalue problem involving the mass and stiffness matrices given in Eq. (6). For $e = 0.01$, the number of reduced eigenvectors $q = 7$ such that $\lambda_1/\lambda_j < \in$. (**a**) Ratio of eigenvalues of the generalised eigenvalue problem. (**b**) Frequency domain response of the tip of the beam under point load for the undamped and damped conditions (constant modal damping)

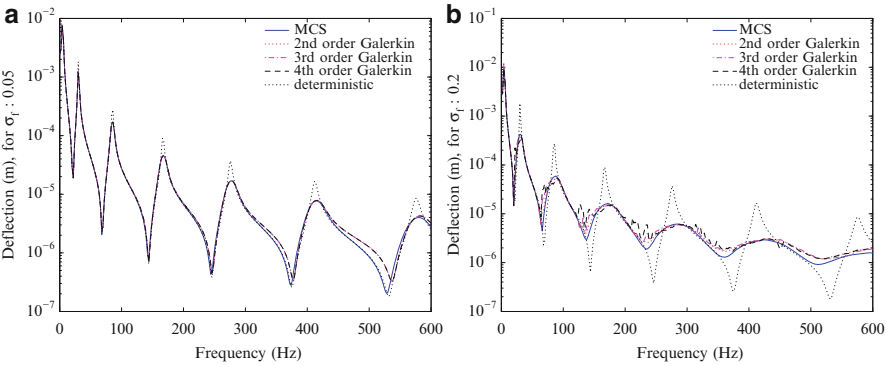

Fig. 2 The frequency domain response of the deflection of the tip of the Euler-Bernoulli beam under unit amplitude harmonic point load at the free end. The response is obtained with 10,000 sample MCS and for $\sigma_a = \{0.05, 0.10, 0.15, 0.20\}$. The proposed Galerkin approach needs solution of a 7×7 linear system of equations only. (**a**) Beam deflection for $\sigma_a = 0.05$. (**b**) Beam deflection for $\sigma_a = 0.2$

The frequency response of the mean deflection of the tip of the beam is shown in Fig. 2 for the cases of $\sigma_a = \{0.05, 0.10, 0.15, 0.20\}$. The figures show a comparison of the direct MCS simulation results with different orders of the solution following Eq. (20), where the orders $s = 2, 3, 4$. A very good agreement between the MCS simulation and the proposed spectral approach can be observed in the figures. All the results have been compared with the response of the deterministic system which shows that the uncertainty has an added damping effect at the resonance peaks. This can be explained by the fact that the parametric variation

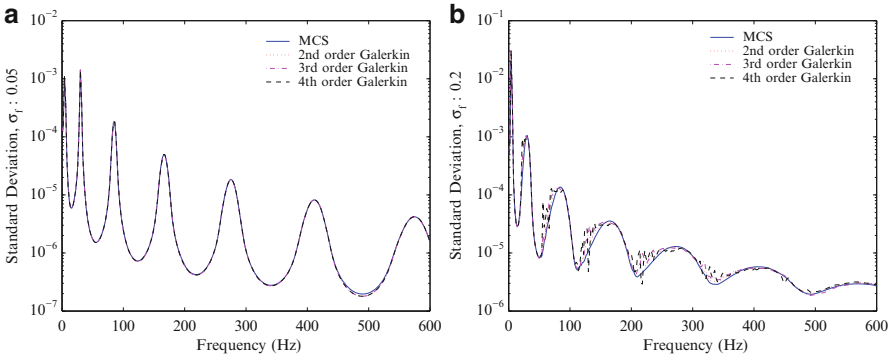

Fig. 3 The standard deviation of the tip deflection of the Euler-Bernoulli beam under unit amplitude harmonic point load at the free end. The response is obtained with 10,000 sample MCS and for $\sigma_a = \{0.05, 0.10, 0.15, 0.20\}$. (**a**) Standard deviation for the reference σ_a=0.05. (**b**) Standard deviation for the reference $\sigma_a = 0.2$

of the beam results in its peak response for the different samples to get distributed around the resonance frequency zones instead of being concentrated at a particular frequency, and when the subsequent averaging is applied, it smoothes out the response peaks to a fair degree. The same explanation holds for the antiresonance frequencies. It can also be observed that increased variability of the parametric uncertainties (as is represented by the increasing value of σ_a) results in an increase of this added damping effect which is consistent with the previous explanation.

The standard deviation of the frequency domain response of the tip deflection for different spectral order of solution of the reduced basis approach is compared with the direct MCS and is shown in Fig. 3, for different values of σ_a. We find that the standard deviation is maximum at the resonance frequencies, which is expected due to the differences in the resonance peak of each sample. It is again observed that the direct MCS solution and the reduced-order approach give almost identical results, which demonstrate the effectiveness of the proposed approach.

The probability density function of the deflection of the tip of the cantilever beam for different degrees of variability of the random field is shown in Fig. 4. The probability density functions have been calculated at the frequency of 412 Hz, which is a resonance frequency of the beam. The results indicate that with the increase in the degree of uncertainty (variance) of the random system, we have long-tailed the density functions which is consistent with the standard deviation curve shown in Fig. 3 and the mean deflection of the stochastic system with the deterministic response in Fig. 2. This shows that the increase in the variability of the stochastic system has a damping effect on the response.

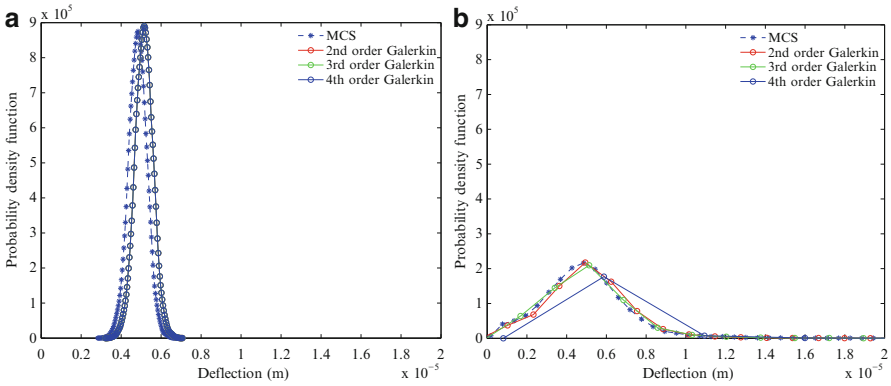

Fig. 4 The probability density function (*PDF*) of the tip deflection of the Euler-Bernoulli beam at 210 Hz under unit amplitude harmonic point load at the free end. The response is obtained with 10,000 samples and for $\sigma_a = \{0.05, 0.10, 0.15, 0.20\}$. (**a**) PDF of the response 210 Hz for $\sigma_a = 0.05$. (**b**) PDF of the response 210 Hz for $\sigma_a = 0.2$

6 Conclusions

Here, we have considered the discretised stochastic partial differential equation for structural systems with generally non-Gaussian random fields. In the classical spectral stochastic finite element approach, the solution is projected into an infinite dimensional orthonormal basis functions, and the associated constant vectors are obtained using the Galerkin type of error minimisation approach. Here an alternative approach is proposed. The solution is projected into a finite dimensional reduced vector basis, and the associated coefficient functions are obtained. The coefficient functions, called as the *spectral functions*, are expressed in terms of the spectral properties of the matrices appearing in the discretised governing equation. It is shown that then the resulting series converge to the exact solution in probability 1. This is a stronger convergence compared to the classical polynomial chaos which converges in the mean-square sense in the Hilbert space. Using an analytical approach, it is shown that the proposed spectral decomposition has the same functional form as the exact solution, which is not a polynomial, but a ratio of polynomials where the denominator has a higher degree than the numerator.

The computational efficiency of the proposed reduced spectral approach has been demonstrated for large linear systems with non-Gaussian random variables. It may be possible to extend the underlying idea to the class of non-linear problems. For example, the proposed spectral approach can be used for every linearisation step or every time step. Further research is necessary in this direction.

Acknowledgement A. Kundu acknowledges the financial support from the Swansea University through the award for Zienkiewicz scholarship. S. Adhikari acknowledges the financial support from the Royal Society of London through the Wolfson Research Merit Award.

References

1. Charmpis DC, Schueeller GI, Pellissetti MF (2007) The need for linking micromechanics of materials with stochastic finite elements: a challenge for materials science. Comput Mater Sci 41(1):27–37
2. Ghanem R, Spanos PD (1991) Stochastic finite elements: a spectral approach. Springer, New York
3. Kelly DW, De SR, Gago JP, Zienkiewicz OC, Babuska I (1983) A posteriori error analysis and adaptive processes in the finite element method: Part I: Error analysis. Int J Numer Methods Eng 19(11):1593–1619
4. Kleiber M, Hien TD (1992) The stochastic finite element method. Wiley, Chichester
5. Matthies HG, Brenner CE, Bucher CG, Soares CG (1997) Uncertainties in probabilistic numerical analysis of structures and solids – stochastic finite elements. Struct Saf 19(3):283–336
6. Nouy A (2007) A generalized spectral decomposition technique to solve a class of linear stochastic partial differential equations. Comput Methods Appl Mech Eng 196(45-48): 4521–4537
7. Nouy A (2008) Generalized spectral decomposition method for solving stochastic finite element equations: invariant subspace problem and dedicated algorithms. Comput Methods Appl Mech Eng 197(51–52):4718–4736
8. Nouy A (2009) Recent developments in spectral stochastic methods for the numerical solution of stochastic partial differential equations. Arch Comput Methods Eng 16:251–285. URL http://dx.doi.org/10.1007/s11831-009-9034-5
9. Stefanou G (2009) The stochastic finite element method: past, present and future. Comput Methods Appl Mech Eng 198(9–12):1031–1051
10. Yamazaki F, Shinozuka M, Dasgupta G (1988) Neumann expansion for stochastic finite element analysis. J Eng Mech ASCE 114(8):1335–1354
11. Zienkiewicz OC, Taylor RL (1991) The finite element method, 4th edn. McGraw-Hill, London